Supporting Information

Redox-controlled self-inclusion of a lasso-type pseudo[1]rotaxane

Hendrik V. Schröder, Jan M. Wollschläger and Christoph A. Schalley*

[a]*Institut für Chemie und Biochemie, Freie Universität Berlin, Takustr. 3, 14195 Berlin, Germany. E-mail: christoph@schalley-lab.de*

Table of contents

1. Experimental details

1.1. General methods

All reagents and solvents were obtained from commercial sources and used without further purification. Dry solvents were purchased from Acros Organics. 4,5-[Naphthalene-1,2-dioxybis(ethane-1,2-diyl)dioxy-bis(ethane-1,2-diyl)dioxybis(ethane-,2-diyl)bisthio]-1,3-dithiole-2-thione **S2**,[1] tert-butyl benzylcarbamate[2] and 3-((5-(methylthio)-2-thioxo-1,3-dithiol-4-yl)thio)propanenitrile[3] were synthesised according to literature procedures. Thin-layer chromatography was performed on silica gel-coated plates with fluorescent indicator F254 (Merck). For column chromatography, silica gel (0.04-0.063 mm, Merck) was used.

^{1}H and ^{13}C NMR experiments were performed on a JEOL ECX 400 or a Bruker AVANCE 700 instruments. Solvent residue signals were used as internal standard. All shifts are reported in ppm and NMR multiplicities are abbreviated as s (singlet), d (doublet), t (triplet), m (multiplet) and br (broad). Coupling constants *J* are reported in Hertz. Compound **2** containing the tetrakis[3,5-bis(trifluoromethyl)phenyl]borate ($BArF_{24}^-$) anion shows a ^{13}C NMR spectra with ^{19}F, ^{10}B and ^{11}B couplings. These signals were denoted as one signal. DOSY measurements were performed on a Bruker AVANCE 500 instrument equipped with a DOSY probe and corresponding gradient amplifier.

High-resolution ESI mass spectra were measured on an Agilent 6210 ESI-TOF device (Agilent Technologies). HPLC grade solvents were used with a flow rate of 2-4 µL/min.

Melting points were determined on a SMP 30 (Stuart) instrument. Melting points are uncorrected.

Redox-potentials were obtained by cyclic voltammetry. All measurements were at least conducted twice. Measurements were carried out in dry and degassed CH_2Cl_2 solutions with 0.1 M NBu_4PF_6 as electrolyte and 1 mM analyte concentration using a three-electrode configuration (freshly polished glassy carbon working electrode, Pt counter electrode, Ag wire as pseudoreference) and an Autolab PGSTAT302N potentiostat. The decamethylferrocene/decamethylferrocenium ($[FeCp_2^*]^{+/0}$) couple was used as the internal reference and the values were referenced against the ferrocene/ferrocenium ($Fc^{+/0}$) couple.[4]

1.2. Synthesis of Boc-protected precursor 1 and lasso 2

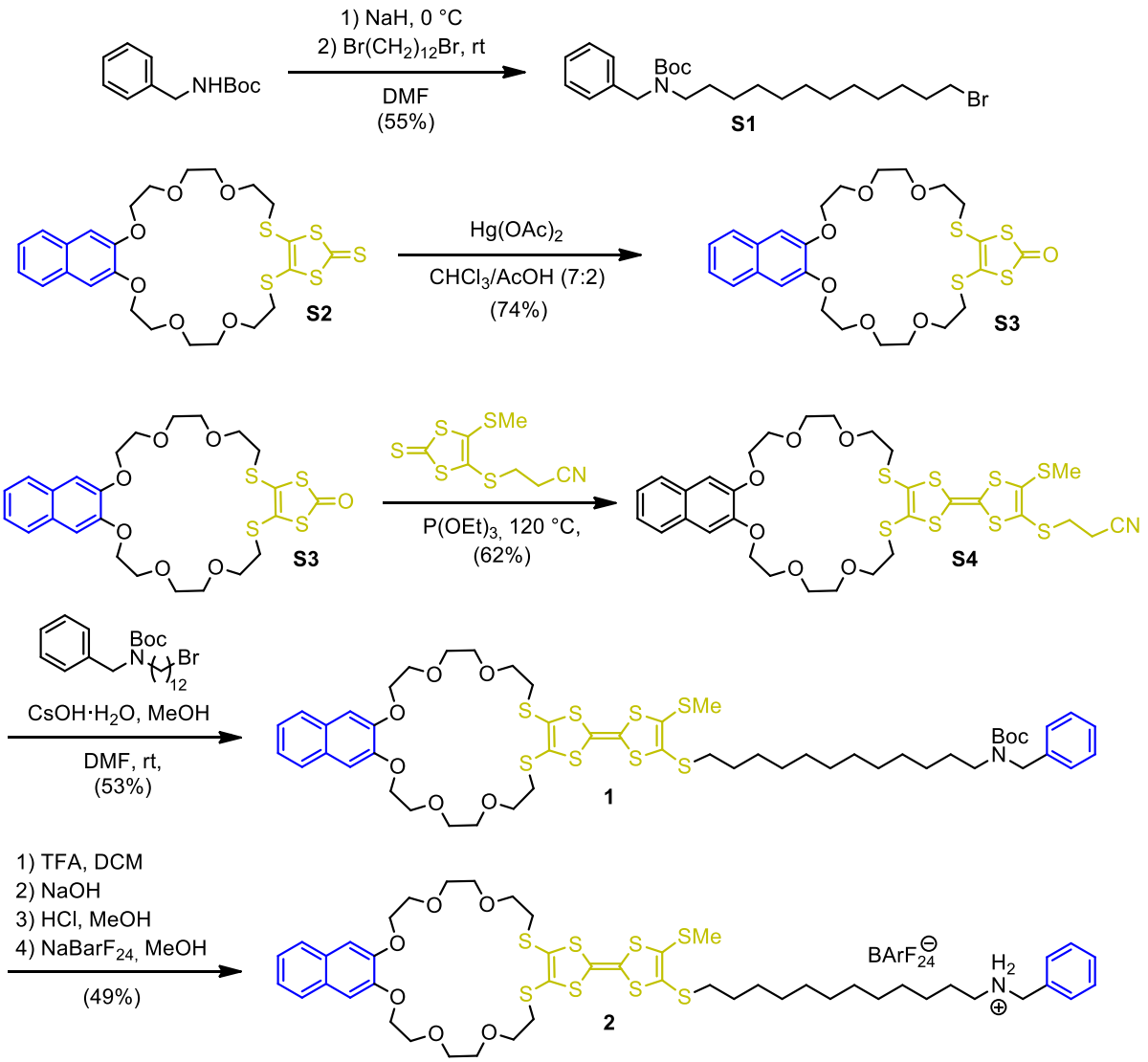

Scheme S1. Synthesis of Lasso **2**

Tert-butyl benzyl(12-bromododecyl)carbamate (S1)

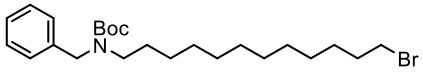

NaH (60 wt% dispersion in oil, 44 mg, 1.1 mmol) was added to a solution of Boc-protected benzylamine (207 mg, 1.0 mmol) in dry dimethylformamide (5 mL) at 0 °C. The solution was warmed to room temperature and stirred for additional 30 min under argon atmosphere. Afterwards, 1,12-dibromododecane (978 mg, 3.0 mmol) was added and the solution was stirred overnight. Residual NaH was quenched by the addition of water (10 mL). The mixture

was extracted with Et_2O (100 mL) and the organic phase was washed with brine (5x100 mL). After drying over $MgSO_4$, the organic phase was concentrated under reduced pressure. The residue was purified by column chromatography (SiO_2, CH_2Cl_2) to yield the desired product as colourless oil (250 mg, 0.55 mmol, 55%). R_f = 0.75 in CH_2Cl_2; ^{1}H NMR (400 MHz, $CDCl_3$, 298 K): δ = 7.65 (m, 2H, H_{Ar}), 7.58 (m, 3H, H_{Ar}), 4.76 (m, 2H, CH_2), 3.75 (t, *J* = 6.9, 2H, CH_2Br), 3.49 (m, 2H, CH_2), 2.19 (p, *J* = 7.0 Hz, 2H, $C\underline{H}_2CH_2Br$), 1.85 - 1.53 (m, 27H, CH_2 & CH_3) ppm; ^{13}C NMR (101 MHz, $CDCl_3$, 298 K): δ = 128.53, 127.80, 127.15, 79.62, 77.16, 34.20, 32.96, 29.68, 29.63, 29.62, 29.54, 29.45, 28.88, 28.58, 28.29, 28.13, 26.96 ppm (only 18 of 20 signals for magnetic inequivalent carbons were observed due to strong signal broadening); HRMS: *m/z* calcd for $[C_{24}H_{40}BrNO_2]$: 476.2135 $[M+Na]^+$, found: 476.2139.

4,5-[Naphthalene-1,2-dioxybis(ethane-1,2-diyl)dioxy-bis(ethane-1,2-diyl)dioxybis(ethane-,2-diyl)bisthio]-1,3-dithiole-2-one S3

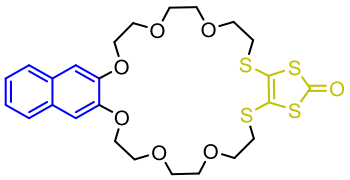

Thione **S2** (115 mg, 0.20 mmol) and $Hg(OAc)_2$ (178 mg, 0.59 mmol) were dispersed in $CHCl_3$/AcOH (5 mL, 7:2) and stirred for 2 days at room temperature. Afterwards, CH_2Cl_2 (50 mL) was added and the organic phase was washed with saturated $NaHCO_3$ solution (50 mL) and brine (2x50 mL). Drying over $MgSO_4$ and concentration under reduced pressure yielded the crude product which was purified by column chromatography (SiO_2, ethyl acetate). The product was obtained as off-white solid (83 mg, 0.15 mmol, 74%). R_f = 0.75 in ethyl acetate; m.p. 116 °C; ^{1}H NMR (400 MHz, CD_2Cl_2, 298 K): δ = 7.68 (m, 2H, H_{Ar}), 7.32 (m, 2H, H_{Ar}), 7.14 (s, 2H, H_{Ar}), 4.24 (m, 4H, CH_2), 3.93 (m, 4H, CH_2), 3.82 - 3.63 (m, 12H, CH_2), 3.05 (m, 4H, CH_2) ppm; ^{13}C NMR (101 MHz, CD_2Cl_2, 298 K): δ = 190.16, 149.53, 129.81, 128.20, 126.74, 124.68, 108.38, 71.45, 71.15, 70.16, 70.10, 69.29, 54.00, 36.77 ppm; HRMS: *m/z* calcd for $[C_{25}H_{30}O_7S_4]$: 593.0766 $[M+Na]^+$, found: 593.0786.

TTF-crown S4

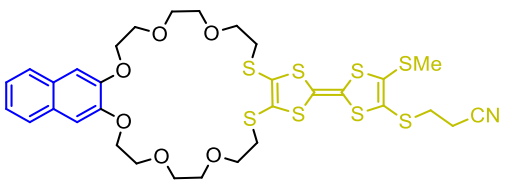

Ketone **S3** (83 mg, 150 µmol) and 3-((5-(methylthio)-2-thioxo-1,3-dithiol-4-yl)thio)propanenitrile (39 mg, 150 µmol) were dispersed in $P(OEt)_3$ (2 mL). The mixture was heated to 120 °C for 1 h. Afterwards, all volatiles were removed *in vacuo* and the residue was purified by column chromatography (SiO_2, CH_2Cl_2 → CH_2Cl_2/MeOH (50:1)). The product was obtained as sticky orange solid (71 mg, 90 µmol, 62%). R_f = 0.40 in CH_2Cl_2/MeOH (50:1); m.p. 109-111 °C; ^{1}H NMR (400 MHz, CD_2Cl_2, 298 K): δ = 7.71 - 7.61 (m, 2H, H_{Ar}), 7.35 - 7.26 (m, 2H, H_{Ar}), 7.13 (s, 2H, H_{Ar}), 4.24 (m, 4H, CH_2), 3.93 (m, 4H, CH_2), 3.81 - 3.61 (m, 12H, CH_2), 3.09 - 2.95 (m, 6H, CH_2), 2.67 (t, ^3J = 7.1, 2H, CH_2), 2.45 (s, 3H, CH_3) ppm; ^{13}C NMR (101 MHz, CD_2Cl_2, 298 K): δ = 149.04, 135.00, 129.33, 128.51, 128.28, 127.72, 126.26, 124.20, 120.37, 117.80, 111.67, 109.95, 107.88, 70.97, 70.89, 70.67, 70.63, 69.77, 69.76, 69.69, 69.68, 69.62, 69.59, 69.58, 68.81, 36.30, 35.76, 31.38, 19.07, 18.76 ppm; HRMS: *m/z* calcd for $[C_{32}H_{37}NO_6S_8]$: 810.0279 $[M+Na]^+$, found: 810.0254.

Boc-protected precursor 1

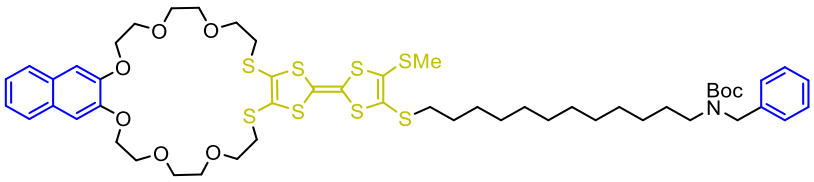

Macrocycle **S4** (70 mg, 89 µmol) was dissolved in dry dimethylformamide (12 mL) and a solution of $CsOHxH_2O$ (16 mg, 93 µmol) in MeOH (1 mL) was added dropwise over a period of 30 min under argon atmosphere. During the addition, the solution changed to dark orange. After stirring for 30 min at room temperature, a solution of tert-butyl benzyl(12-bromododecyl)carbamate (162 mg, 355 µmol) was added dropwise over 30 min. The mixture was stirred for additional 2 h and was concentrated under reduced pressure afterwards. The residue was dissolved in CH_2Cl_2 (50 mL) and washed with brine (3x50 mL). After drying over $MgSO_4$, the organic phase was evaporated *in vacuo* and the crude product was purified by column chromatography (SiO_2, CH_2Cl_2 → CH_2Cl_2/MeOH (150:1)). The desired product was obtained as sticky orange oil (52 mg, 47 µmol, 53%). R_f = 0.25 in CH_2Cl_2/MeOH (150:1); ^{1}H NMR (400 MHz, CD_2Cl_2, 298 K): δ = 7.67 (m, 2H, H_{Ar}), 7.35 - 7.28 (m, 4H, H_{Ar}), 7.26 - 7.19 (m, 3H, H_{Ar}), 7.13 (s, 4H, H_{Ar}), 4.40 (s, 2H, CH_2), 4.26 - 4.13 (m, 4H, CH_2), 3.93 (m, 4H, CH_2), 3.78 (m, 4H, CH_2), 3.71 - 3.60 (m, 8H, CH_2), 3.12 (br, 2H, CH_2), 3.00 (t, ^3J = 6.2 Hz, 4H, CH_2), 2.81 (m, 27H, CH_2 & H_{Boc}) ppm; ^{13}C NMR (176 MHz, CD_2Cl_2, 298 K): δ = 149.61, 129.91, 129.88, 128.89, 128.85, 127.99, 127.72, 127.46, 126.78, 126.46, 124.70, 111.73, 110.42, 108.48, 79.66, 71.44, 71.13, 70.33, 70.32, 70.14, 70.12, 69.37, 54.00, 47.19, 36.83, 36.28, 30.28,

30.12, 30.07, 29.92, 29.67, 28.98, 28.72, 27.39, 19.58 ppm; HRMS: *m/z* calcd for $[C_{53}H_{73}NO_8S_8]$: 1130.2994 $[M+Na]^+$, found: 1130.3037.

Pseudo[1]rotaxane 2

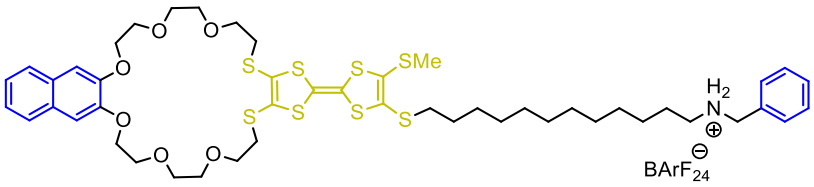

Boc-protected precursor **1** (11.1 mg, 10.0 µmol) was dissolved in trifluoric acid/CH_2Cl_2 (1:20, 2 mL). The mixture turned dark brown and was stirred for 6 h under argon atmosphere at room temperature. Afterwards, the mixture was diluted with CH_2Cl_2 (20 mL) and washed with aqueous NaOH solution (1 M, 3x20 mL). The organic phase was dried over $MgSO_4$ and concentrated *in vacuo* to yield the free amine which was used without further purification. The amine was dissolved in tetrahydrofuran/MeOH (1:5, 2 mL) and aqueous HCl (1 M) was added dropwise to adjust a pH < 2. The mixture was stirred for 3 h at room temperature and concentrated under reduced pressure afterwards. MeOH (2 mL) and sodium tetrakis[3,5-bis(trifluoromethyl)phenyl]borate (8.86 mg, 10.0 µmol) were added and the mixture was stirred for another 2h. After concentration *in vacuo*, the residue was purified by preparative thin layer chromatography (SiO_2, 0.5 mm diameter, CH_2Cl_2/MeOH (250:1)) to obtain the desired product as orange oil (9.2 mg, 4.9 µmol, 49%). R_f = 0.80 in CH_2Cl_2/MeOH (250:1); ^{1}H NMR (700 MHz, CD_2Cl_2, 298 K): δ = 7.72 (br, 10H, H_{BArF24} & H_{Ar}), 7.56 (s, 4H, H_{BArF24}), 7.52-7.48 (m, 2H, H_{Ar}), 7.41 (m, 2H, H_{Ar}), 7.31- 7.24 (m, 3H, H_{Ar}), 7.14 (m, 2H, H_{Ar}), 4.68 (m, 2H, NCH_2), 4.26 (m, 4H, OCH_2), 3.91-3.50 (m, 16H, OCH_2), 3.41 (m, 4H, CH_2 & OCH_2), 3.21i (m, 4H, OCH_2), 2.78 (m, 2H, CH_2), 2.42 (s, 3H, CH_3), 1.64 (m, 2H, CH_2), 1.56 (m, 2H, CH_2), 1.30 (m, 20H, CH_2) ppm; ^{13}C NMR (176 MHz, CD_2Cl_2, 298 K): δ = 162.31, 147.46, 135.37, 132.21, 130.32, 130.26, 129.80, 129.71, 129.71, 129.43, 127.49, 127.41, 127.00, 126.98, 126.78, 125.84, 125.82, 125.18, 118.03, 114.58, 111.04, 110.59, 108.92, 108.88, 71.73, 71.68, 71.43, 71.13, 70.82, 70.72, 70.69, 70.54, 69.47, 69.30, 54.00, 53.49, 50.10, 37.40, 37.16, 36.02, 30.60, 30.27, 30.18, 30.08, 29.57, 29.54, 28.66, 28.45, 27.01, 26.96, 19.72 ppm; HRMS: *m/z* calcd for $[C_{80}H_{78}BF_{24}NO_6S_8]$: 1008.2650 $[M-BArF_{24}]^+$, found: 1008.2642.

2. 2D NMR spectra and DOSY measurements

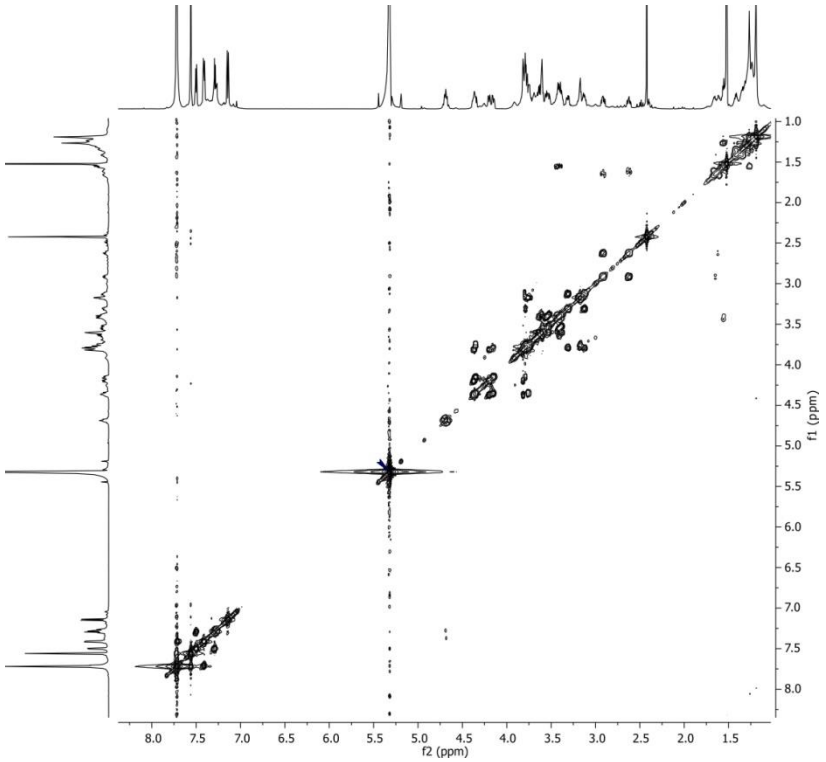

Fig. S1 $^{1}H,^{1}H$ COSY NMR (700 MHz, CD_2Cl_2, 2 mM, 298 K) of pseudo[1]rotaxane **2**.

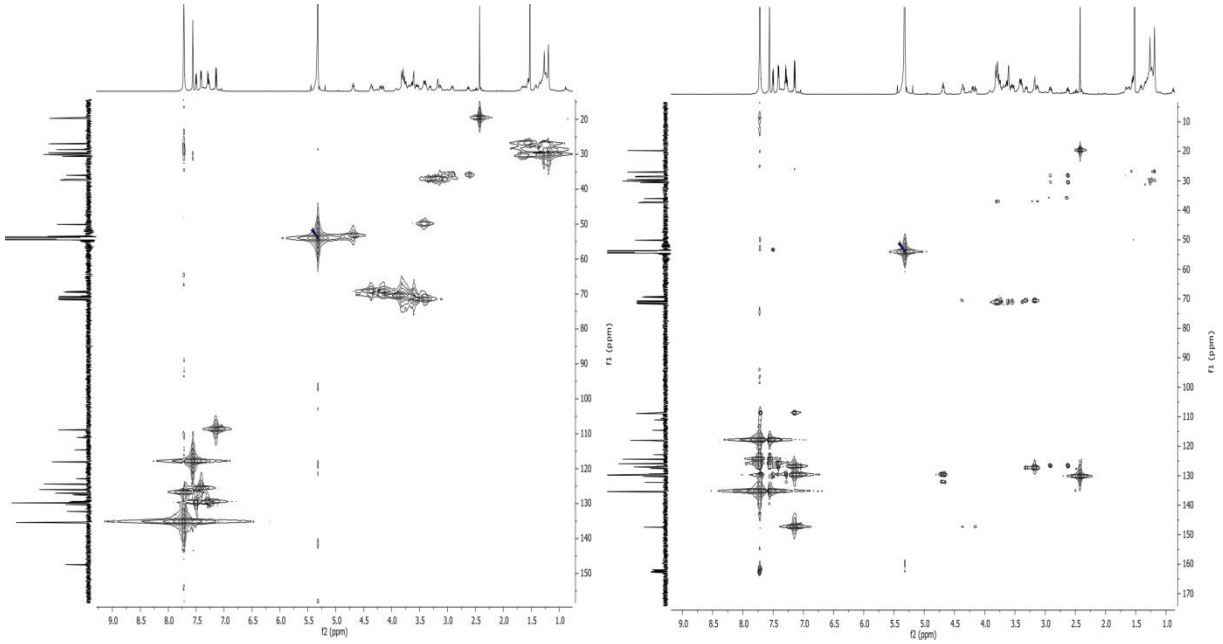

Fig. S2 (left) $^{1}H,^{13}C$ HMQC and (right) $^{1}H,^{13}C$ HMBC NMR (700/176 MHz, CD_2Cl_2, 2 mM, 298 K) of pseudo[1]rotaxane **2**.

DOSY measurements

DOSY measurements were performed twice. To ensure reliable measurements dimethyl sulfoxide (1 µL) was added as reference for the second measurement. The data were processed and plotted (Fig. 2 in the main text) with the Bruker TopSpin Software. The diffusion coefficient D_0 was determined by fitting the diffusion decays of three integrals (see the data below) and averaging over these values. The error corresponds to the standard deviation obtained from the different integrals. The hydrodynamic radius R_H (Stokes radius) was calculated by the Stokes-Einstein equation. The structures in figure S3 were modelled with the MMFF94 force field method implemented in the Avogadro[5] program package. R_H and D_0 of the modelled structures were estimated by using the Connolly solvent excluded volume and the Stokes-Einstein equation. The Connolly solvent excluded volume was calculated with Chem3D (CambridgeSoft).

Integral 1 (64 points)
Integral Region from 7.873 to 7.675 ppm
Results Comp. 1
I[0] = 3.944e-02
Diff Con. = 7.778e-10 m^2 s^{-1}
Gamma = 4.258e+03 Hz/G
Little Delta = 4.500m
Big Delta = 22.310m

Integral 2 (64 points)
Integral Region from 7.564 to 6.946 ppm
Results Comp. 1
I[0] = 2.896e-02
Diff Con. = 7.638e-10 m^2 s^{-1}
Gamma = 4.258e+03 Hz/G
Little Delta = 4.500m
Big Delta = 22.310m

Integral 3 (64 points)
Integral Region from 4.020 to 3.272 ppm
Results Comp. 1
I[0] = 4.192e-02
Diff Con. = 6.885e-10 m^2 s^{-1}
Gamma = 4.258e+03 Hz/G
Little Delta = 4.500m
Big Delta = 22.310m

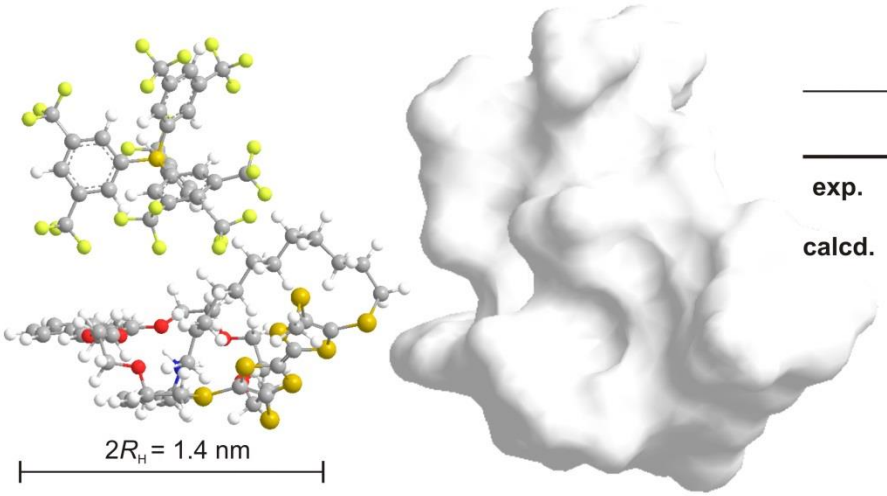

	D_0 / 10^{-10} m^2 s^{-1}	R_H / nm
exp.	7.43	0.70
calcd.	7.51	0.71

Fig. S3 Calculated structures of pseudo[1]rotaxane **2** (MMFF94) with and without Connolly surface and corresponding experimental and calculated R_H and D_0 values.

3. Electrochemistry and digital simulations

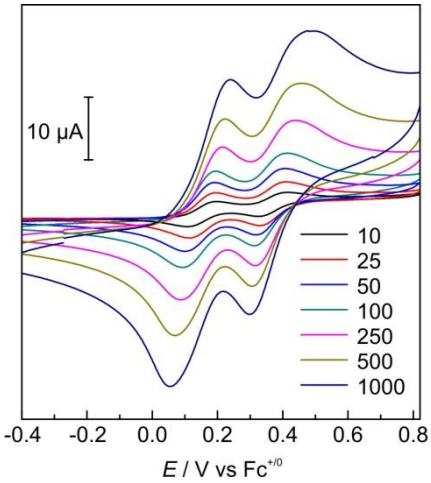

Fig. S4 Cyclic voltammograms at different scan rates (10→1000 mV s^{-1}, CH_2Cl_2, 1 mM, 298 K) of pseudo[1]rotaxane **2** with NBu_4PF_6 (0.1 M) as electrolyte.

The cyclic voltammogram of **2** was simulated in two segments with the software DigiElch Professional[6] by using the Butler-Volmer equation. The surface area of the working electrode was set to 0.02 cm^2 and the starting concentration of **2** was set to 1 mM. The charge-transfer coefficients α were at the initial value of 0.5 and the heterogeneous rate constants k_s were set to 0.015 $cm^2\ s^{-1}$. The diffusion coefficients were set to 7.43×10^{-10} $m^2\ s^{-1}$ (see DOSY experiments in the main text). According to the square scheme (fig. 3c), we assumed four electrochemical (E1-E4) and three chemical (C1-C3) reactions. The oxidation potentials for *non-threaded*-**2** are given by the potentials of precursor **1** which displayed no significant axle-wheel interaction. Due to prior dethreading, the second oxidation potential $E^2_{1/2}$ of *threaded*-**2** was not accessible by CV. We used the previously reported potential of a structural similar [2]rotaxane since a dethreading can be excluded here.[7] The experimental data were fitted over several scan rates (Fig. S4) to obtain the parameters in table S1. The intramolecular equilibrium ratio K_n is definded by K_n = [*threaded*-2^{n+}]/[*non-threaded*-2^{n+}]. Since several assumptions were made (e.g. coefficients α, electrode surface area and the heterogeneous rate constants k_s) in the fitting and simulation process, these values should be considered as estimations.

threaded-**2**	⇌	*threaded*-$\mathbf{2}^{\bullet+}$	(0.13 V)	(E1)
threaded-$\mathbf{2}^{\bullet+}$	⇌	*threaded*-$\mathbf{2}^{2+}$	(0.39 V)	(E2)
non-threaded-**2**	⇌	*non-threaded*-$\mathbf{2}^{\bullet+}$	(0.05 V)	(E3)
non-threaded-$\mathbf{2}^{\bullet+}$	⇌	*non-threaded*-$\mathbf{2}^{2+}$	(0.33V)	(E4)

threaded-**2** ⇌ *non-threaded*-**2** (C1)

threaded-**2**$^{\bullet+}$ ⇌ *non-threaded*-**2**$^{\bullet+}$ (C2)

threaded-**2**$^{2+}$ ⇌ *non-threaded*-**2**$^{2+}$ (C2)

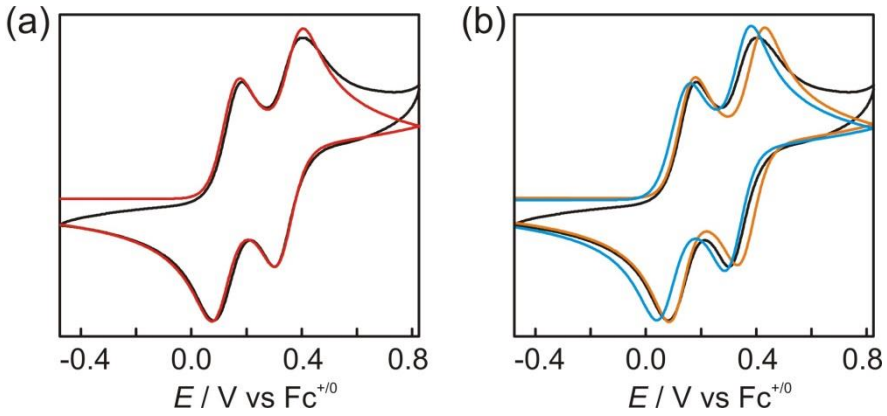

Fig. S5 (a) (black trace) Experimental (100 mV s^{-1}, CH_2Cl_2, 1 mM, 298 K) with NBu_4PF_6 (0.1 M) as electrolyte and (red) simulated voltammogram with parameters in table S1 of pseudo[1]rotaxane **2**. (b) Simulations with K_n values divided (blue curve) or multiplied (orange curve) with a factor of 10 to illustrate the impact of K_n on the simulated data. The clear differences to the experiment illustrate that the values in table S1 are reasonable estimates.

Table S1. Thermodynamic and kinetic values for reactions C1-C3 derived by fitting the experimental data by a computational model and used for the simulation of cyclic voltammograms depicted in Fig. S5.

reaction	K_n	k_f / s^{-1}	k_b / s^{-1}
C1	40	5	0.14
C2	2	130	67
C3	0.2	200	1200

4. NMR experiments and chemical switching

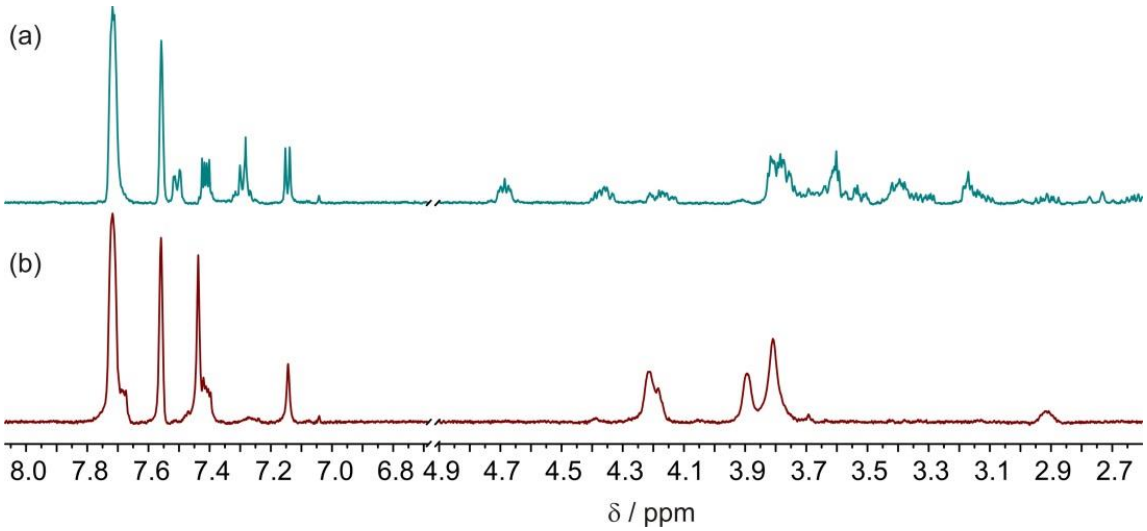

Fig. S6 Partial ^{1}H NMR spectra (400 MHz, CD_2Cl_2, 0.5 mM, 298 K) of pseudo[1]rotaxane **2** (a) before and (b) after chemical oxidation by two equivalents of $Fe(ClO_4)_3 \cdot H_2O$. The strong signal broadening in (b) is likely caused by paramagnetic traces of the radical cation $\mathbf{2}^{\bullet+}$.

5. IM-MS experiments

ESI-MS measurements and traveling-wave ion mobility mass spectrometry (IM-MS) experiments were performed on a Synapt G2-S HDMS (Waters Co., Milford, MA, USA) instrument. The experimental conditions including flow rate (10 µL min^{-1}), spray voltage (3.6 kV), source temperature (80 °C), sample cone voltage (30 V) and source offset of (39 V) were kept constant during the measurements. The desolvation temperature was set to 320 °C. Samples were diluted to a concentration of 0.1 µM in CH_2Cl_2.

For preparation of $\mathbf{2}^{\bullet+}$ and $\mathbf{2}^{2+}$, pseudo[1]rotaxane **2** was chemically oxidised in CH_2Cl_2 solutions with $Fe(ClO_4)_3 \cdot H_2O$ by stirring the suspension for several minutes. $Fe(ClO_4)_3 \cdot H_2O$ shows very low solubility in CH_2Cl_2 and can be filtered off after oxidation. The deprotonated potassium adduct of **2** ($[\mathbf{2}+K\text{-}HBArF_{24}]^+$) was generated by dissolving **2** (0.1 mM) in MeOH/NEt_3 (100:1, 100 µL), addition of KPF_6 (100 equiv.) and dilution (10^4 fold) by CH_2Cl_2.

Collision Induced (CID) tandem MS experiments were conducted with nitrogen as collision gas in the trap cell (i.e. before the IMS cell) with trap voltages between 0 and 60 eV. For IM-MS measurements, the IMS Wave velocity was set to 652 m s^{-1}, the IMS wave height to 40.0 V, the transfer wave height to 4.0 V and the IMS gas flow (nitrogen) to 90.00 mL min^{-1}, respectively.

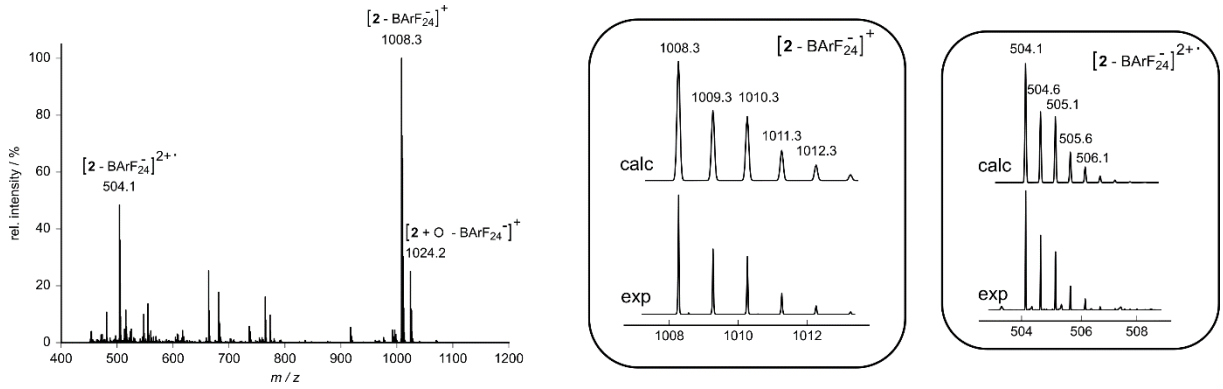

Fig. S7 ESI mass spectrum of **2** (0.1 µM, CH_2Cl_2) with experimental and calculated isotopic distributions of signals *m/z* 1008 and *m/z* 504.

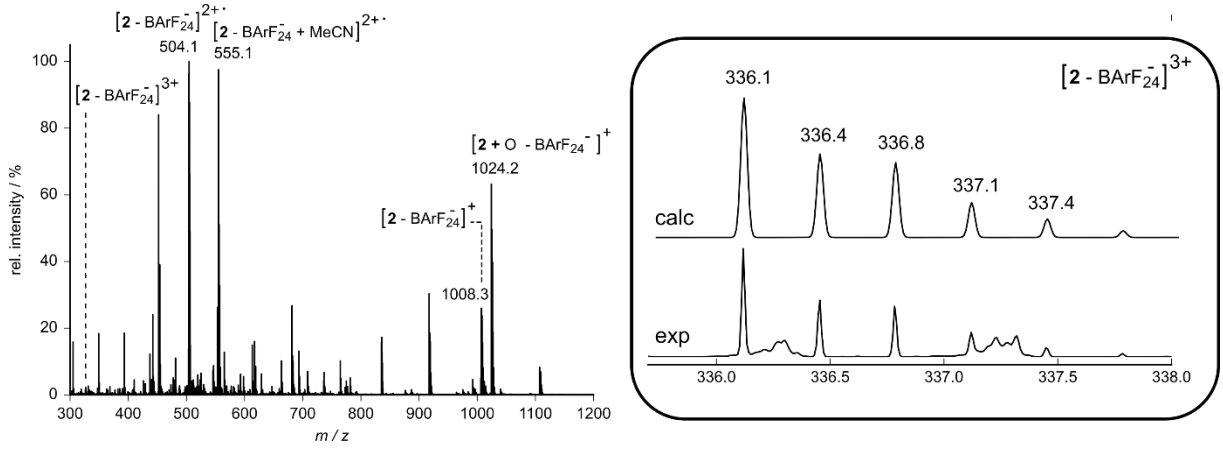

Fig. S8 ESI mass spectrum of **2** (0.1 µM, CH_2Cl_2) after chemical oxidation by $Fe(ClO_4)_3 \cdot H_2O$ and isotopic distribution of signal *m/z* 336 corresponding to doubly oxidised **2**.

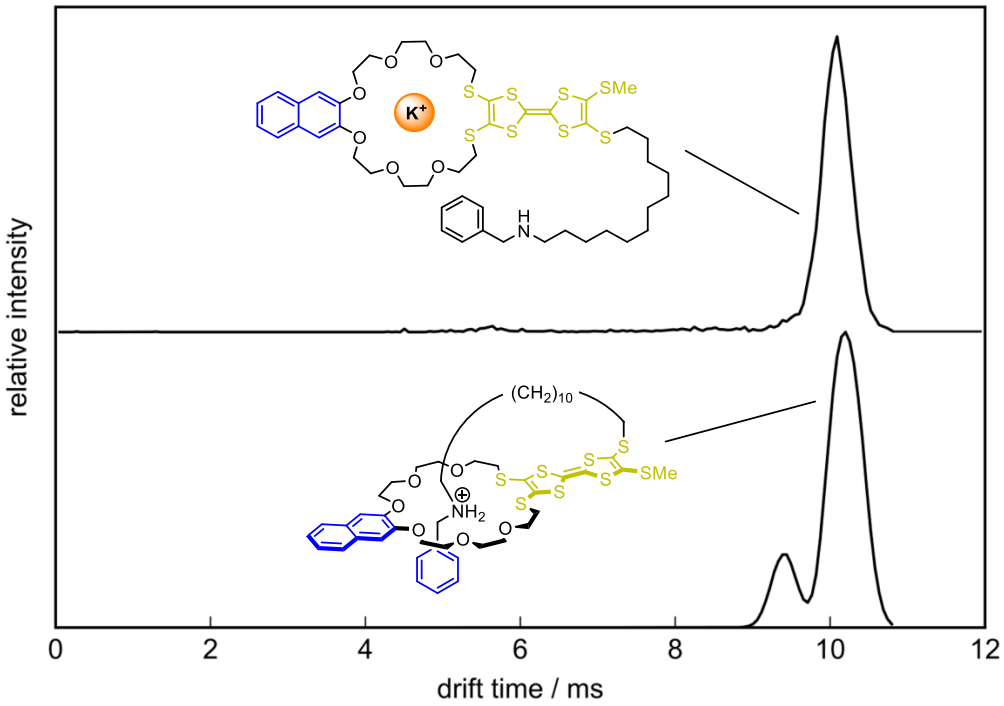

Fig. S9 IM-MS experiments with pseudo[1]rotaxane **2** (0.1 µM, CH_2Cl_2): Comparison of ATD for (top) the deprotonated potassium adduct [**2**+K-HBArF$_{24}$]$^+$ (*m/z* 1046) and (bottom) [**2**-BArF$_{24}$]$^+$ (*m/z* 1008). Since the axle is deprotonated and the potassium ion occupies the crown, a fully non-threaded state can be assumed for [**2**+K-HBArF$_{24}$]$^+$. However, the complexation of the potassium ion prevents, analogous to the axle threading, a folding of the crown. Therefore, the signal for the threaded isomer of [**2**-BArF$_{24}$]$^+$ and [**2**+K-HBArF$_{24}$]$^+$ display a very similar drift time in the ATD. This shows that the major conformational difference between the isomers (threaded/non-threaded) in **2** is indeed the folding of the unoccupied crown.

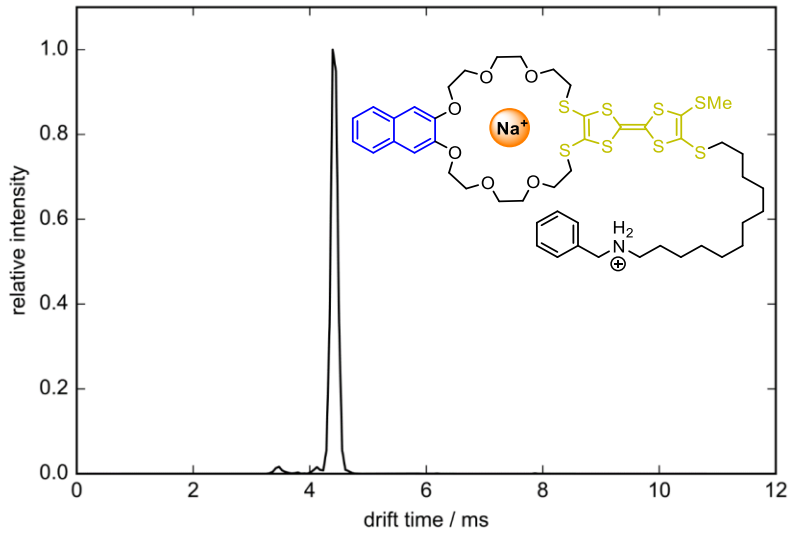

Fig. S10 IM-MS experiment of **2** (0.1 µM, CH_2Cl_2). Shown is the ATD of signal *m/z* 515 corresponding to [**2**+Na-$BArF_{24}$]$^{2+}$. Most likely, the sodium ion occupies the crown and competes with the axle as guest. Therefore, only a single peak is observed since the threaded/non-threaded ratio is completely shifted to the non-threaded isomer. Note that the arrival times depend on the charge state and thus shorten for the 2+ species.

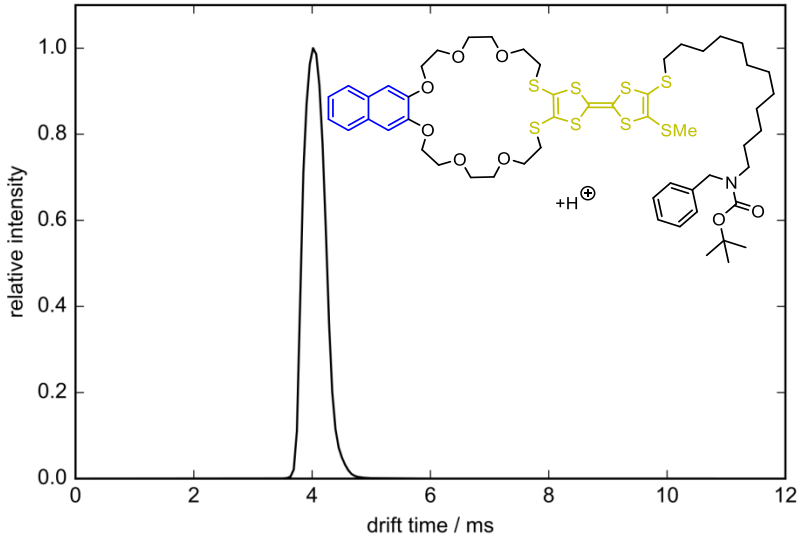

Fig. S11 IM-MS experiment of Boc-protected precursor **1** (0.1 µM, CH_2Cl_2). Shown is the ATD of signal *m/z* 1108 corresponding to [**1**+H]$^+$. Only a single peak is observed, as no axle threading is present. This additionally confirms that the threading/dethreading process is mandatory for the isomer signals in the ATD of **2**. Note that the IMS gas flow (nitrogen) was adjusted from 90.00 to 57.00 mL min^{-1} due to technical reasons. This leads to an overall shorter drift time which cannot compared with the drift times above.

6. NMR spectra

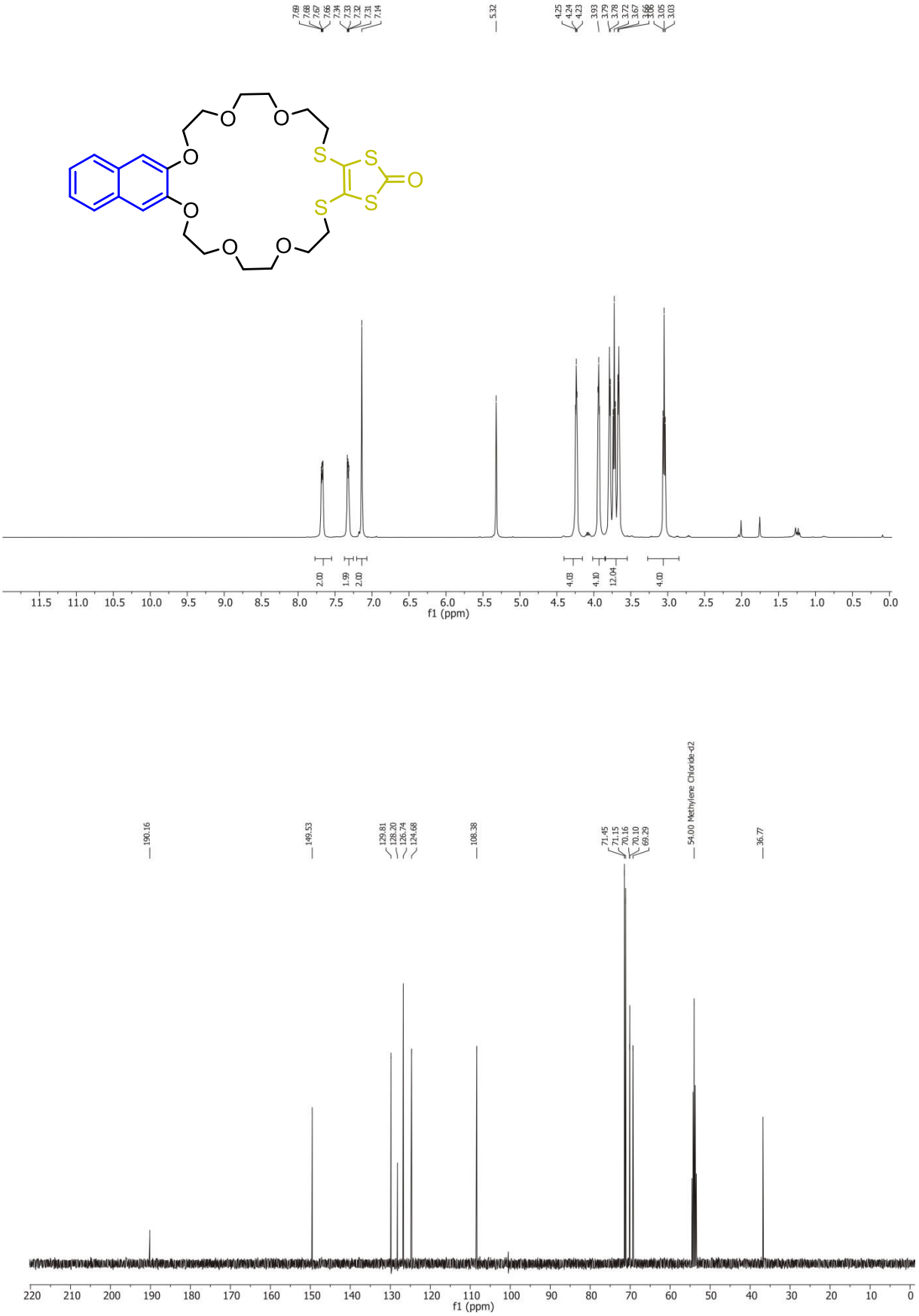

Fig. S12 (top) ^{1}H and (bottom) ^{13}C NMR spectra (400/101 MHz, CD_2Cl_2, 298 K) of **S3.**

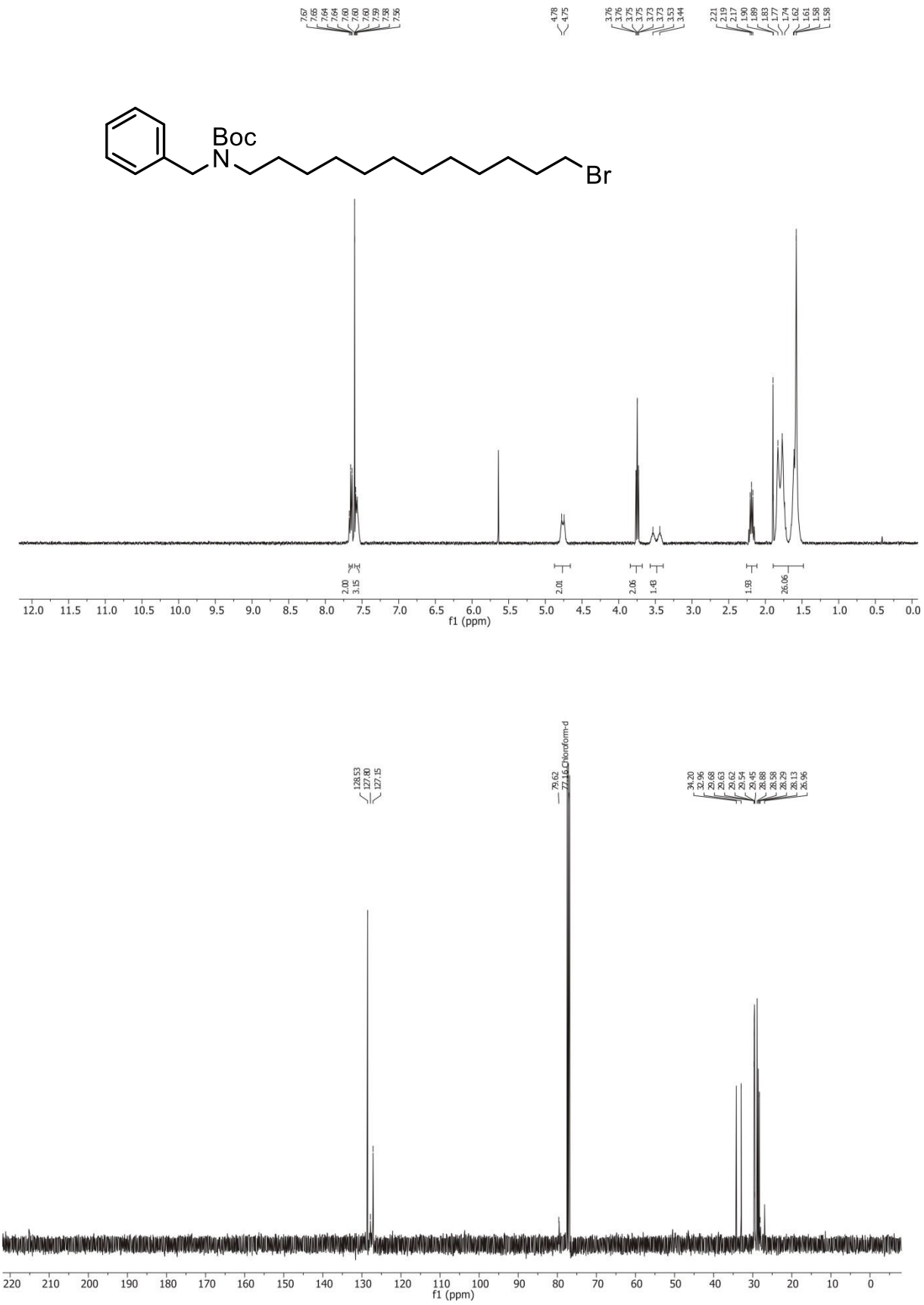

Fig. S13 (top) ^{1}H and (bottom) ^{13}C NMR spectra (400/101 MHz, $CDCl_3$, 298 K) of **S1.**

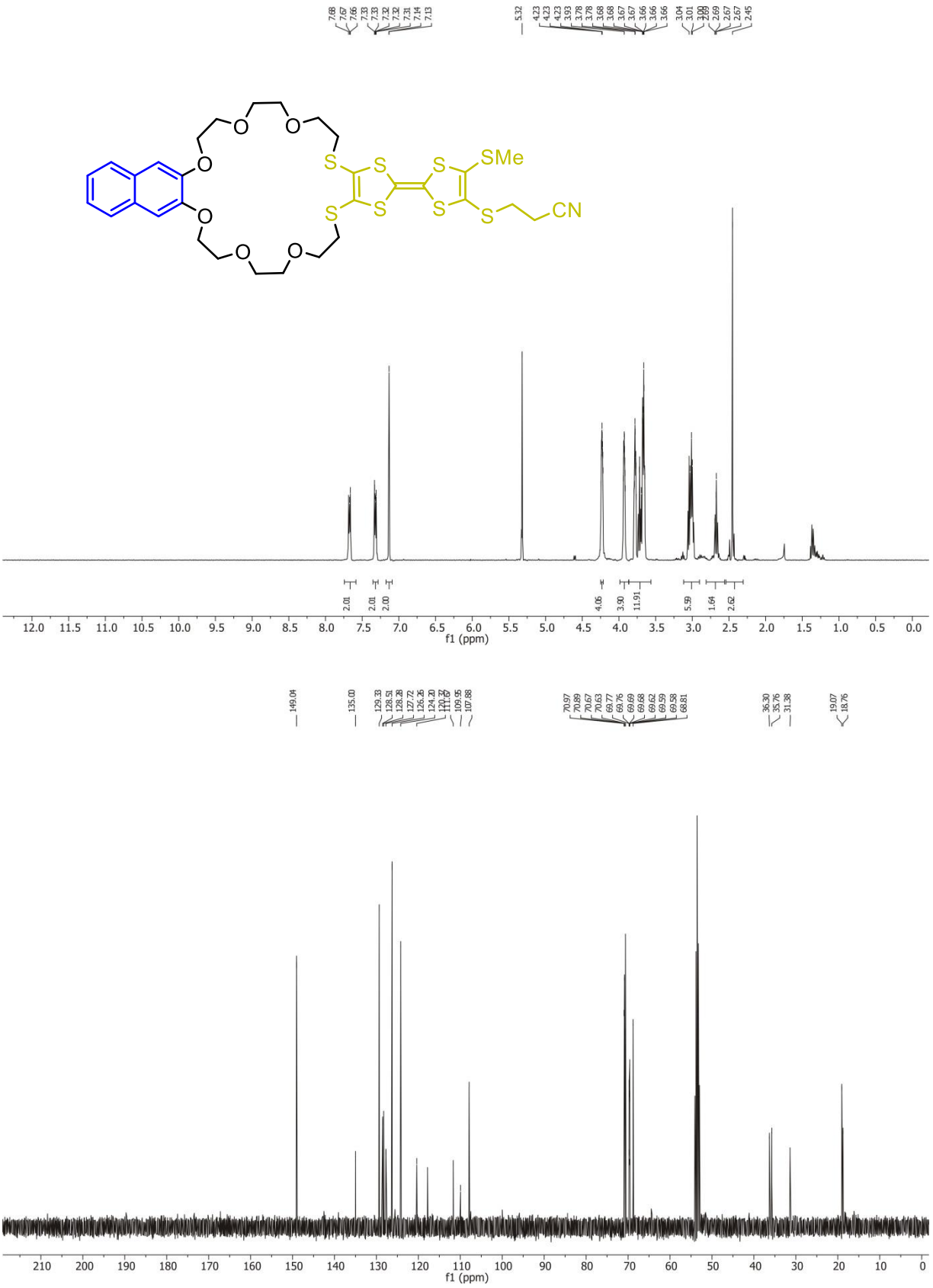

Fig. S14 (top) ^{1}H and (bottom) ^{13}C NMR spectra (400/101 MHz, CD_2Cl_2, 298 K) of **S4.**

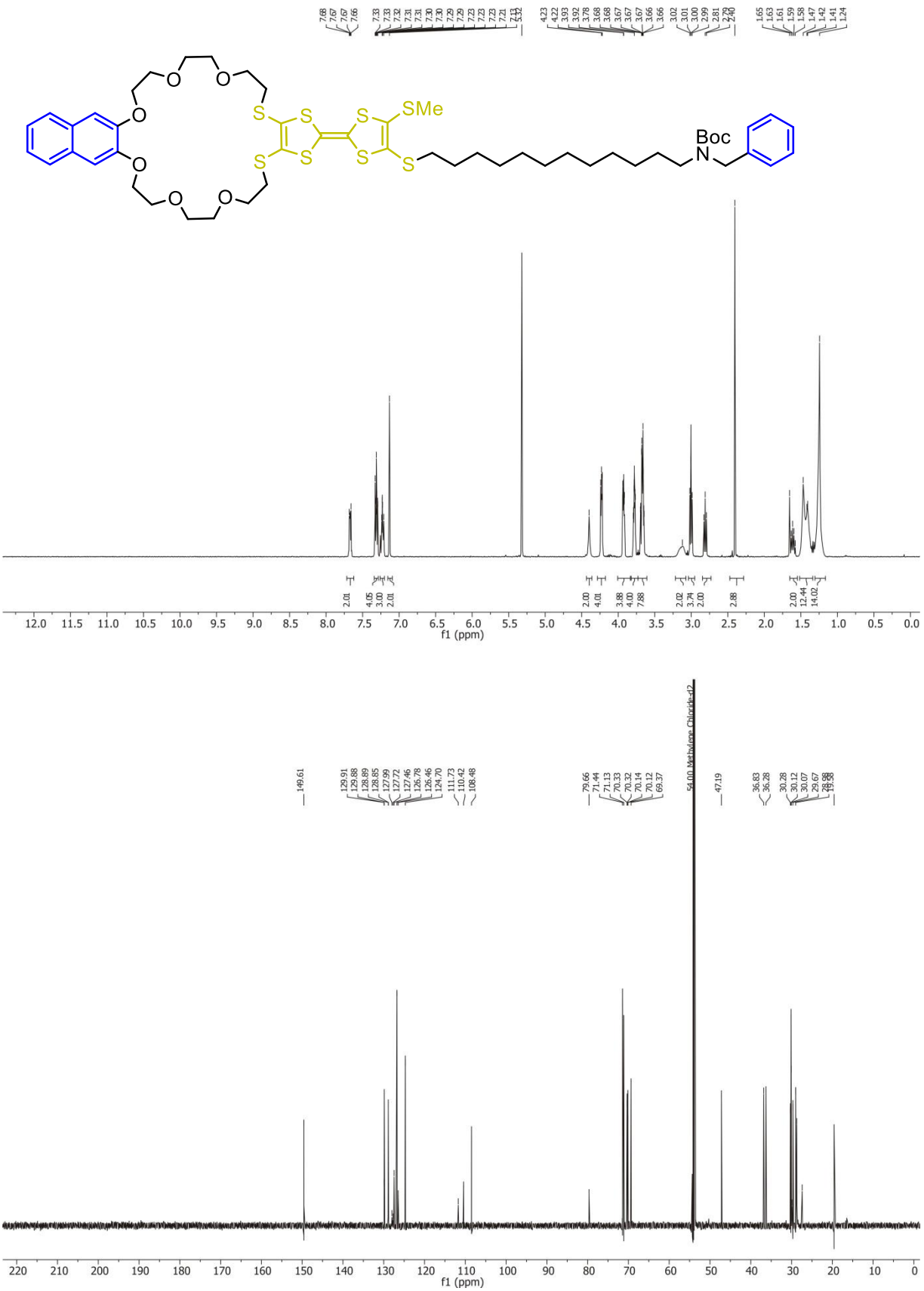

Fig. S15 (top) ^{1}H and (bottom) ^{13}C NMR spectra (400/176 MHz, CD_2Cl_2, 298 K) of **1.**

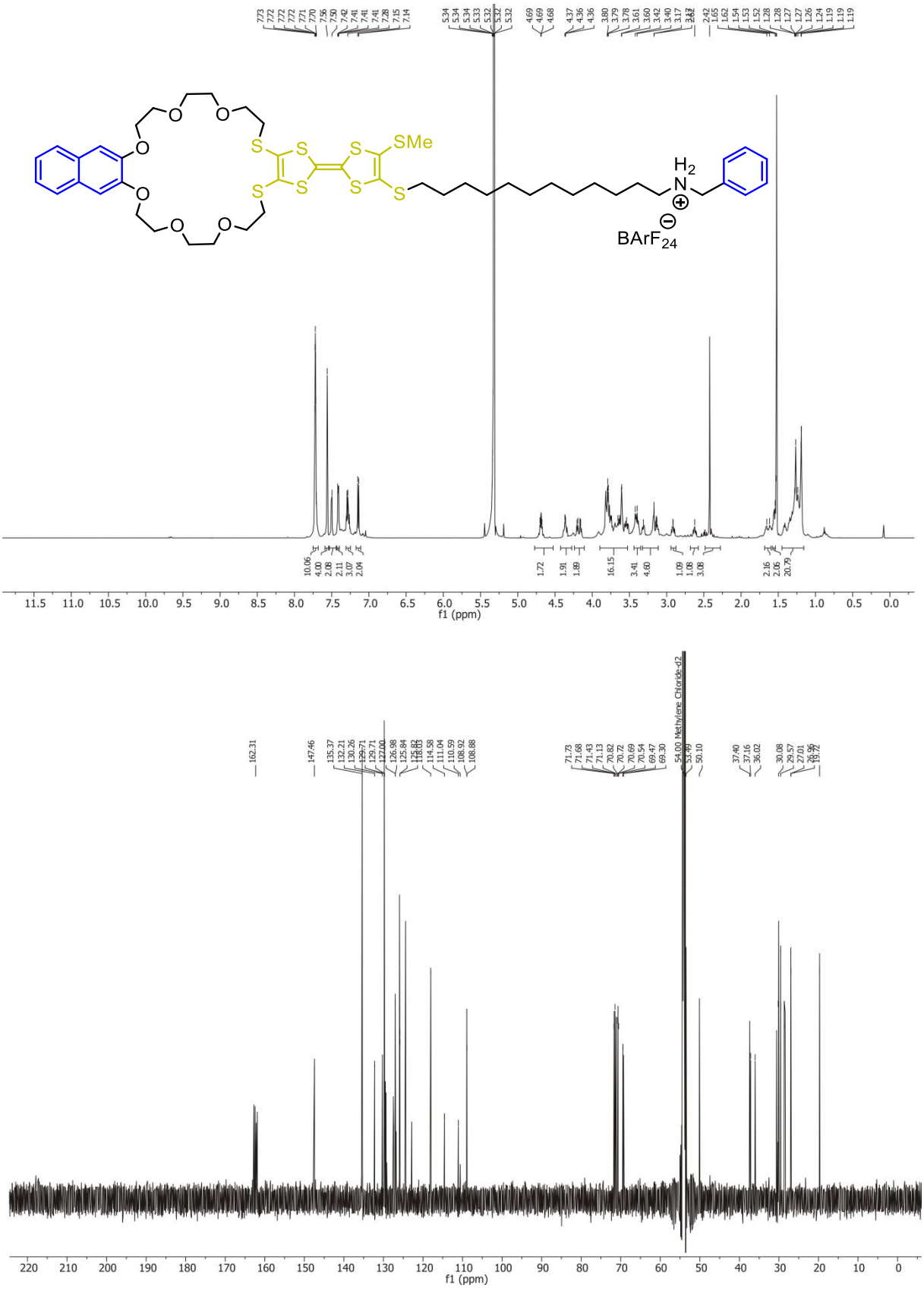

Fig. S16 (top) ^{1}H and (bottom) ^{13}C NMR spectra (700/176 MHz, CD_2Cl_2, 298 K) of **2.**

7. Mass spectra

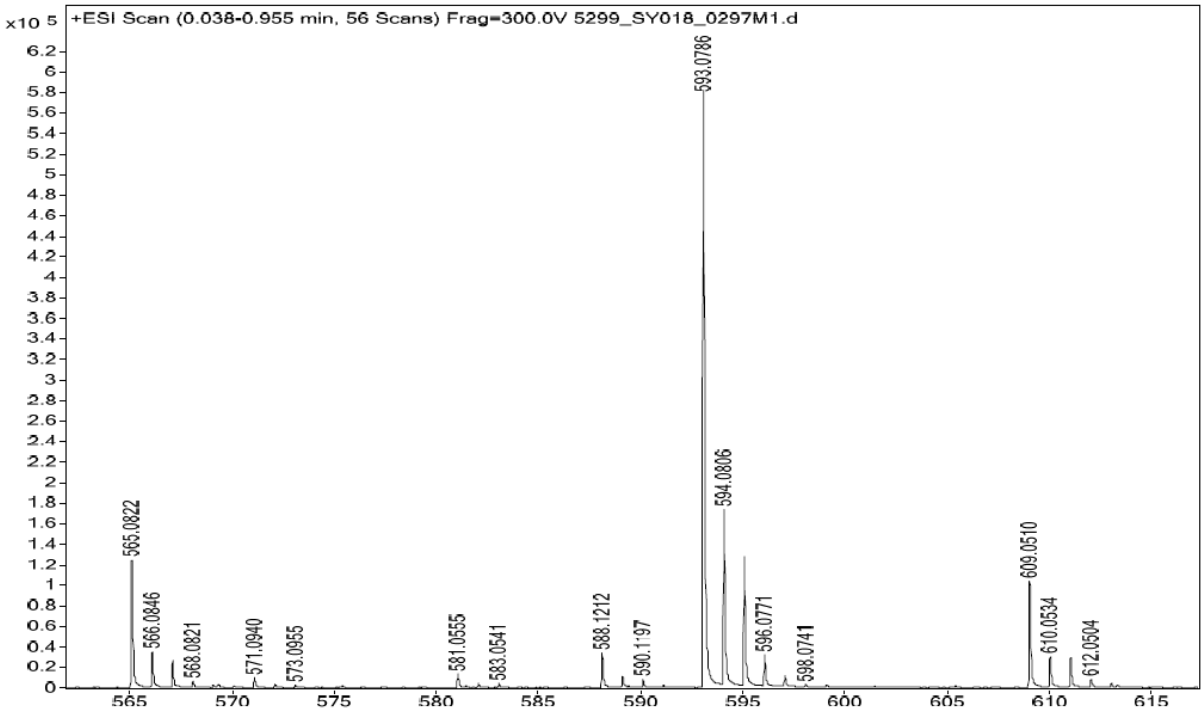

Fig. S17 ESI mass spectrum (MeOH, positive mode) of **S3**

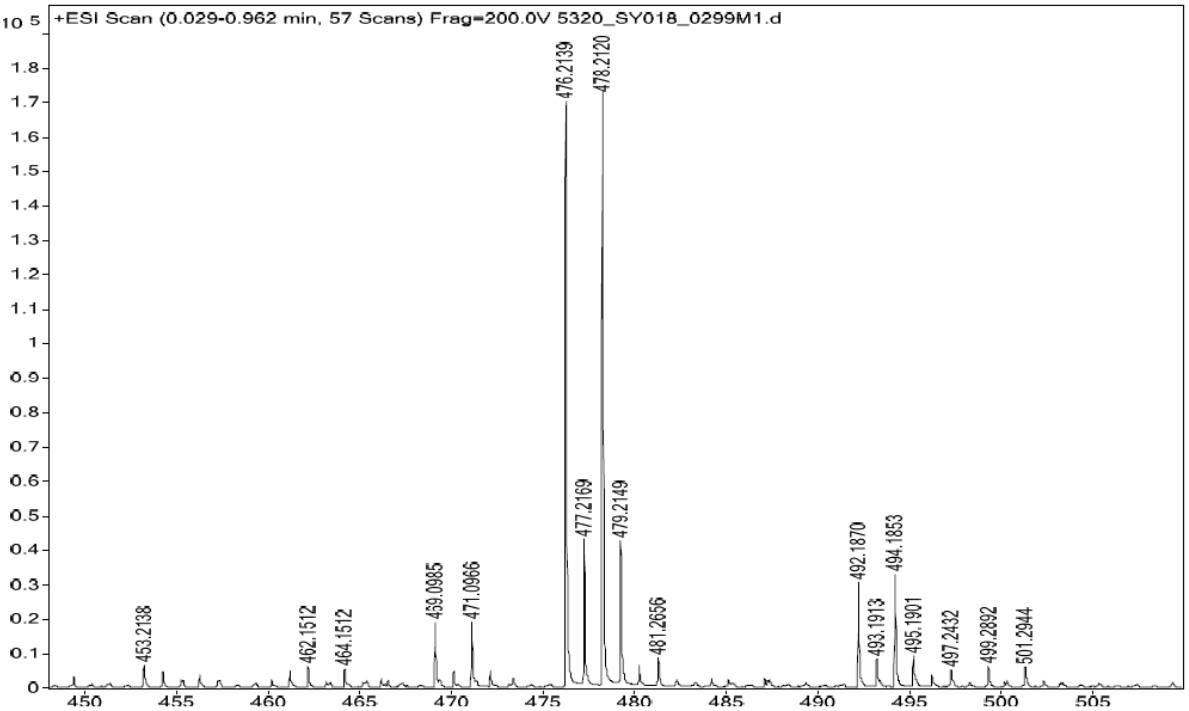

Fig. S18 ESI mass spectrum (MeOH, positive mode) of **S1**.

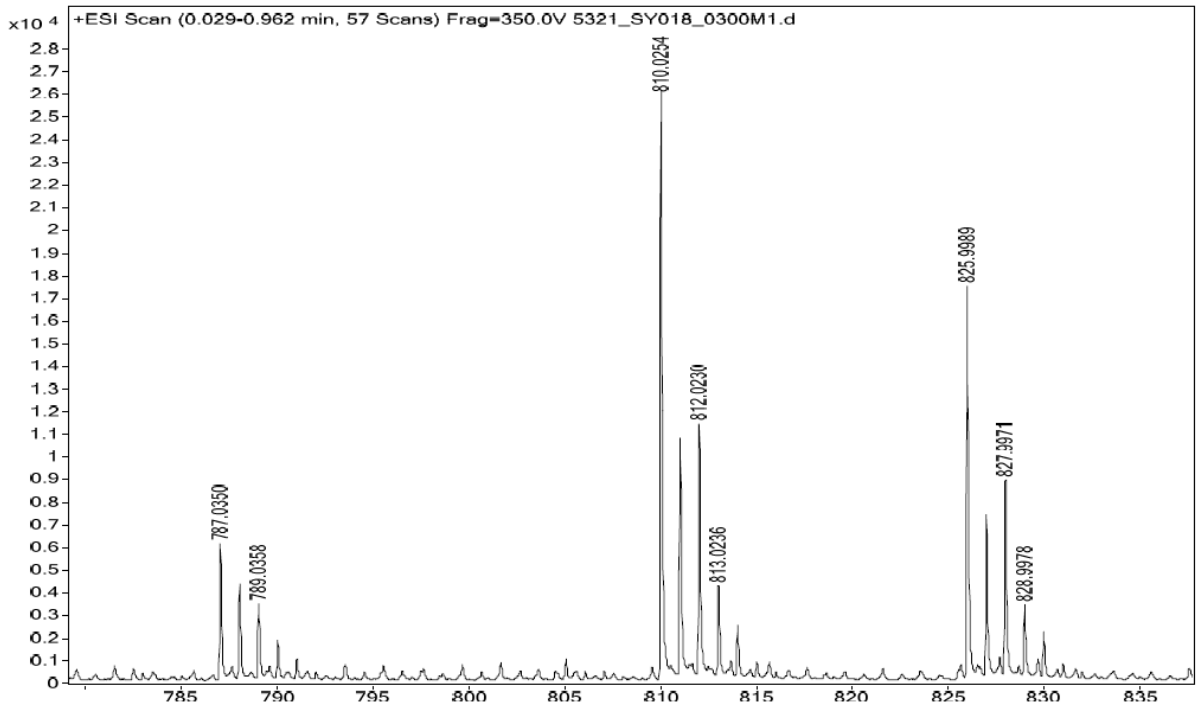

Fig. S19 ESI mass spectrum (MeOH, positive mode) of **S4**.

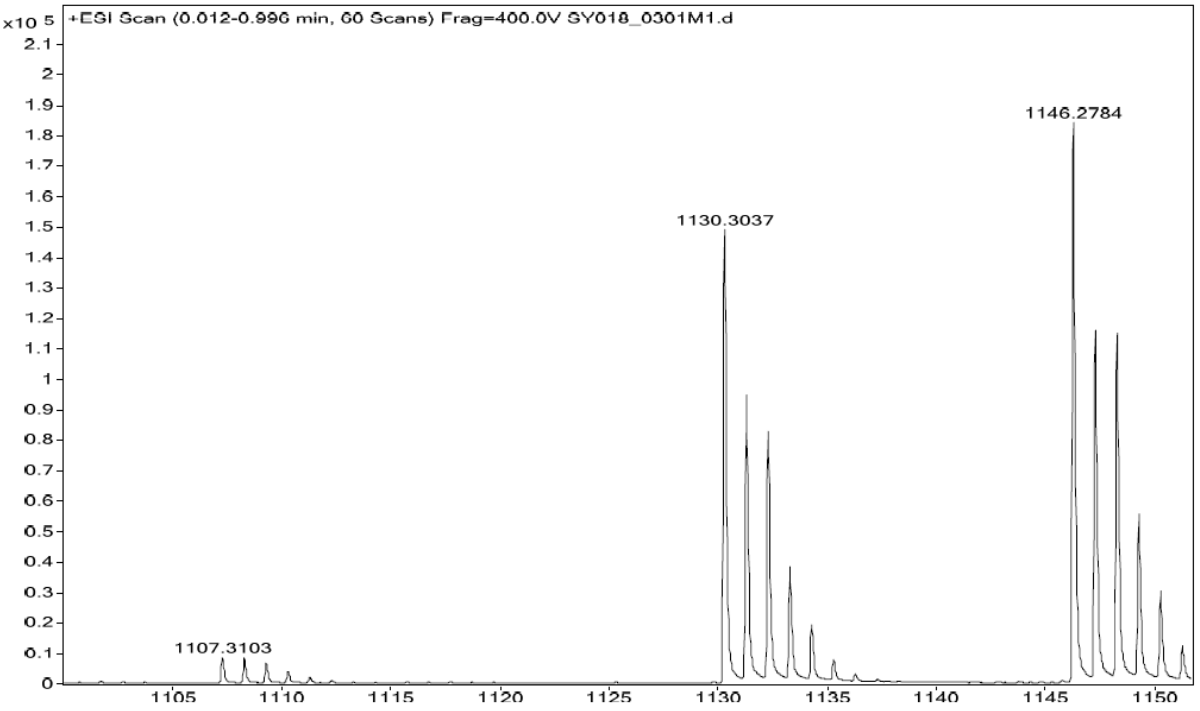

Fig. S20 ESI mass spectrum (MeOH, positive mode) of **1**.

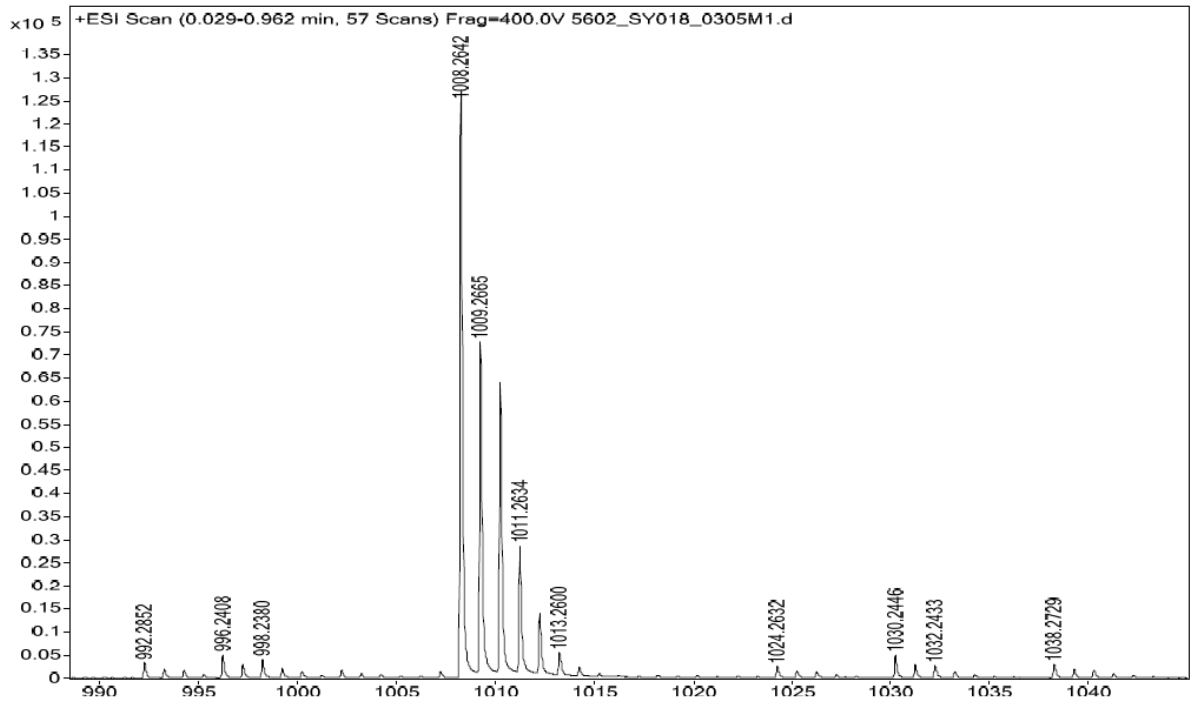

Fig. S21 ESI mass spectrum (MeOH, positive mode) of **2**.

8. References

1 H. V. Schröder, H. Hupatz, A. J. Achazi, S. Sobottka, B. Sarkar, B. Paulus and C. A. Schalley, *Chem. Eur. J.*, 2017, **23**, 2960-2967.

2 A. M. Kanazawa, A. Correa, J. N. Denis, M. J. Luche and A.E. Greene, *J. Org. Chem.*, 1993, **58**, 255-257.

3 K. B. Simonsen, N. Svenstrup, J. Lau, O. Simonsen, P. Mørk, G. J. Kristensen and J. Becher, *Synthesis*, 1996, **3**, 407-418.

4 J. R. Aranzaes, M.-C. Daniel, and D. Astruc, *Can. J. Chem.*, 2006, **84**, 288–299.

5 M. D. Hanwell, D. E. Curtis, D. C. Lonie, T. Vandermeersch, E. Zurek and G. R Hutchison, *J. Cheminform.*, 2012, *4*, 17.

6 DigiElch Professional Version 7.FD 2006, ElchSoft GbR, Kleinromstedt, Germany.

7 H. V. Schröder, S. Sobottka, M. Nößler, H. Hupatz, M. Gaedke, B. Sarkar and C. A. Schalley, *Chem. Sci.*, 2017, in press.